Angular Distribution of Protons Measured by the Energetic Particle Telescope on PROBA-V

Stanislav Borisov, Sylvie Benck, Mathias Cyamukungu, *Member, IEEE*, Paul O'Brien, Joseph Mazur, Petteri Nieminen, Hugh Evans, and Eamonn Daly

***Abstract*—Angular distribution and contamination of proton spectra measured at LEO are considered as possible sources of discrepancies between fluxes obtained by different instruments. In particular, not accounted for pitch angle distribution and East/West asymmetry of energetic proton fluxes have been suspected of leading to the reported underestimates of these fluxes by the NASA Model AP8. The energetic particle telescope (EPT) was designed as a science-class instrument aimed at providing uncontaminated fluxes of electrons ($0.5 - 20$ MeV), protons ($9.5 - 300$ MeV) and α-particles ($38 - 1200$ MeV) getting into the instrument from within a well-defined Field Of View (FOV). The PROBA-V satellite with EPT was launched on May 7th, 2013 on a LEO, 820 km altitude, 98.7° inclination and a 10:30–11:30 Local Time at Descending Node. Based on the data acquired by the EPT on board PROBA-V, we account for flux angular distribution effects to provide a definitive reply to the basic question: "does AP8 underestimate $E > 100$ MeV proton fluxes around $B/B_0 = 1.1, L = 1.3$"?**

***Index Terms*—AP8, Energetic Particle Telescope, EPT, energetic protons, pitch angle distribution, radiation belts, space radiation environment, space radiation model.**

I. Introduction

PROTON flux models developed during the last two decades have challenged the general applicability of AP8 model considered as a de-facto standard until then. These new models include the Trapped Proton Model (TPM) [1], [2] based on TIROS satellite data and the PSB97 model [3] based on SAMPEX/PET data, both of which are credited for being built from high quality data sets. The energy and position coverage of these models are different, but the apparent overestimate of unidirectional $E > 100$ MeV proton fluxes (extrapolated in case of TPM) below 1000 km altitude relative to AP8 predictions is a common feature that was suspected to result from the assumption of isotropy in the conversion process from AP8 omnidirectional fluxes to their unidirectional counterpart [4]. Through the use of AP8 omnidirectional fluxes combined with Badhwar-Konradi (BK) Pitch Angle Distribution (PAD) model [5], Siegl *et al.* [6] have been able to predict proton-induced counts recorded in channel TC2 (E $>$ 49 MeV) by the SREM radiation monitor on board PROBA-1 (PRoject for On Board Autonomy–1). For that energy range, Siegl *et al.* [6] even concluded that AP8 overestimated the fluxes within L coordinates in the 1.3–1.6 range. Of course, prediction of counts for channel C3 (76 MeV $< E <$ 450 MeV) and channel C4 ($E >$ 164 MeV) would have brought complementary information on AP8 applicability, since it is mainly at highest proton energies that AP8 is reported to underestimate fluxes even as an omnidirectional flux model [2], [3]. However, the above-mentioned PROBA-1/SREM data analysis methodology clearly indicated that angular distributions of particle fluxes have to be accounted for in thorough validation of AP8 as well as in any development of a radiation environment model for LEO. This requirement was one of the key elements accounted for during the elaboration of the PROBA-V/EPT data exploitation plan. PROBA-V being a three-axis stabilized satellite, it was not planned to measure angular distributions of proton fluxes at every position along the S/C orbit, but only to target a position in space (hereunder also called *"reference position" or "RP"*) where the EPT boresight direction would be modified in a way leading to a complete pitch angle distribution data set at the end of the commissioning phase. Such a measurement has been performed and was complemented by that of proton fluxes at two azimuths (East and West) in the RP bin: $-56° \pm 2°$ longitude, $-20° \pm 2°$ latitude, 828 km altitude (centered at $L = 1.27$ and $B = 0.165$). Proton fluxes measured at high latitude during Solar Particle Events (SPE) have also been analyzed for angular distribution assessment. Based on the observed performances of the EPT including its angle selection capabilities and the conclusions of the angular distribution study, we have devised a clear methodology for cross-comparison of the fluxes measured by the EPT with those from the Relativistic Particle Spectrometer (RPS) on board the Van Allen Probes (abbreviated RBSP for historical reasons). Furthermore, we have drawn conclusions on AP8 capability to predict fluxes of $E > 100$ MeV protons in the RP bin.

The EPT instrument along with the PROBA-V satellite is briefly presented in Section II. The measurements of proton PAD (including Solar Energetic Protons (SEP)) performed during the EPT commissioning phase are described in Section III, whereas the asymmetry observed on the proton flux

Manuscript received June 27, 2014; revised September 01, 2014; accepted October 04, 2014. Date of publication December 04, 2014; date of current version December 11, 2014. This work was supported by the Belgian Science Policy under ESA/PRODEX PEA 4000107617.

S. Borisov, S. Benck, and M. Cyamukungu are with the University of Louvain-la-Neuve (UCL/CSR), Chemin du Cyclotron, 2 B-1348 Louvain-la-Neuve, Belgium (e-mail: Stanislav.Borisov@uclouvain.be).

P. O'Brien and J. Mazur are with the Aerospace Corporation, Chantilly, VA 20151 USA (e-mail: Paul.OBrien@aero.org).

P. Nieminen, H. Evans, and E. Daly are with the European Space Agency (ESA) Keplerlaan, 1 2201 AZ Noordwijk, Netherlands (e-mail: Petteri.Nieminen@esa.int).

Digital Object Identifier 10.1109/TNS.2014.2361951

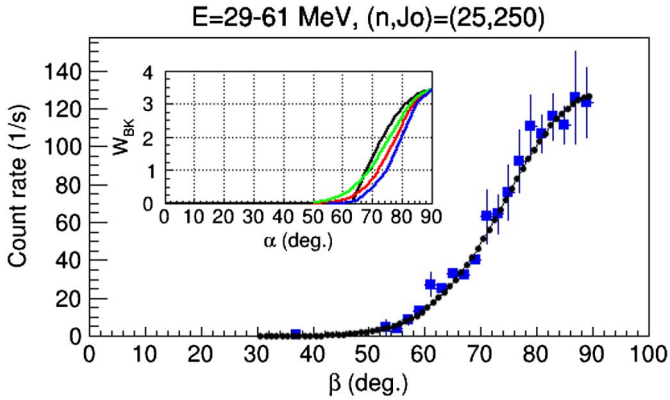

Fig. 1. Count rate in the EPT proton channel 29–61 MeV as a function of the boresight orientation β (blue squares) and counts prediction based on the best fit PAD model (black circles). The inset shows the Badhwar-Konradi scaling factor (black line) W_{BK} for the RP. The red and green lines show the normalized PAD of the form $\sin^n(\alpha)$ with $n = 25$ and $n = 18$ respectively. The blue line in the inset represents the shape of AP9 pitch angle distribution for 40 MeV protons.

distribution in a plane perpendicular to local magnetic field is analyzed in Section IV. The cross-comparison of EPT results and RPS-based predictions is provided in Section V, which also contains AP8 flux predictions for the RP. Finally, a concluding Section VI summarizes our methodology and the answer to our basic question.

II. The EPT Instrument on Board PROBA-V

The satellite PROBA-V was launched on the 7th May 2013 onto a sun-synchronous circular Low Earth Orbit at 820 km altitude and 98.7° inclination. Its local time at descending node is 10:30–11:30. The EPT is a science-class particle spectrometer that is capable to measure uncontaminated energy spectra of electrons (0.5–20 MeV), protons (9–300 MeV) and He-ions (38–1200 MeV) within a 52° Field Of View (FOV) angle and a 149 cm^2sr aperture geometrical factor. The instrument is modular and it can be in-flight configured so as to provide up to 19 energy channels per particle type. The EPT dimensions are 210 mm × 162 mm × 128 mm, the total mass is 4.6 kgs and its power consumption amounts to 5.6 Watts [7]. The EPT has been accommodated onto the PROBA-V satellite so as to get its boresight oriented Eastwards during local night time and Westwards during local day time. However, the East/West orientation has been modified by telecommands during the commissioning phase to allow measurements of PAD.

III. PAD of Proton Fluxes Measured by PROBA-V/EPT

Measurements of proton fluxes in off-pointing conditions were performed from June 25th, 2013 to December 10th, 2013. The experiment protocol was that PROBA-V was rotated northwards from its nominal attitude, before flights in the RP bin in the South Atlantic Anomaly (SAA). The rotation angles were in the 0° to 45° range and allowed to cover boresight orientations with respect to the magnetic field (β) from 30° to 90° (after setting the equivalence $\beta \equiv 180° - \beta$ for β values exceeding 90°). A typical result of count rates measurement as a function of EPT boresight orientation β is shown in Fig. 1.

The PAD for 29–61 MeV protons was assumed to be of the form $J(\alpha) = J_0 \sin^n(\alpha)$ and the model parameters, n and J_0, were extracted through a process that starts by the evaluation of the EPT aperture gathering power as a function of n and the boresight orientation with regards to local magnetic field, β. Then, the instrument efficiency is evaluated as a function of n and β, after which the counts can be calculated and compared to predictions based on candidate model parameters. The details of this analysis procedure are described in the Appendix. Despite the limited number of passes across the RP bin during the three months of EPT commissioning activities, values of n were found to be in the 18–25 range for all energy channels, whereas J_0 follows the energy spectrum shape and is equal to 7.8 protons/(cm^2s sr MeV) for the 29–61 MeV channel in the RP bin, with an uncertainty of the order of 15%. The value of n obtained by the above-described PAD fitting procedure are compatible with the results from the evaluation of Badhwar-Konradi scaling factor W_{BK} [8] as shown in the inset of Fig. 1, although the PAD cut at loss cone angle is smoother as expected from a $J(\alpha) \sim \sin^n(\alpha)$ model and from an experimental procedure.

The PAD of proton fluxes measured during SPE has been separately investigated. The current results are compatible with a rather isotropic angular distribution of fluxes measured in the polar horns around May 22nd, June 22nd, 2013 and January 8th, 2014. In fact, taking an example of the January 8th, 2014 SPE, it is seen on Fig. 2, that while the pitch-angle varies by ∼ 30° (from 117° down to 87°), from 11:50 to 12:06 UTC, the flux of protons remains constant. This kind of isotropy of solar energetic protons at $L > 4$ values has been reported in [9] along with a clear statement of their importance in instrument intercalibration.

IV. Azimuthal Distribution of Proton Fluxes

As it crosses the SAA, the EPT boresight is either towards East (night crossings) or towards West (day crossings). The count rates measured in both conditions are shown in Fig. 3 for $\beta = 90°$.

The count rates and fluxes for protons from West (red rounds) are higher than their East-coming counterparts. However, the difference induced by the well-known East-West effect decreases with decreasing magnetic latitudes. The EPT did not measure fluxes at $\beta = 90°$ during its day-time passes across the RP around $B/B_0 = 1.1$, but it can be assumed that performing the PAD measurements exclusively during night time did not affect the resulting parameters. In fact, while an order of magnitude difference between East and West proton fluxes can be encountered at $B/B_0 \sim 1.3$ it can be noticed that this difference decreases with decreasing B/B_0, to an extent it disappears as soon as interaction with upper atmosphere is no longer affecting the proton motion [10]. Thereby, the azimuthal angular distribution of proton fluxes in the RP bin ($B/B_0 \sim 1.1$) cannot be invoked to explain discrepancies (if any) between AP8 and EPT measurements in that bin [9].

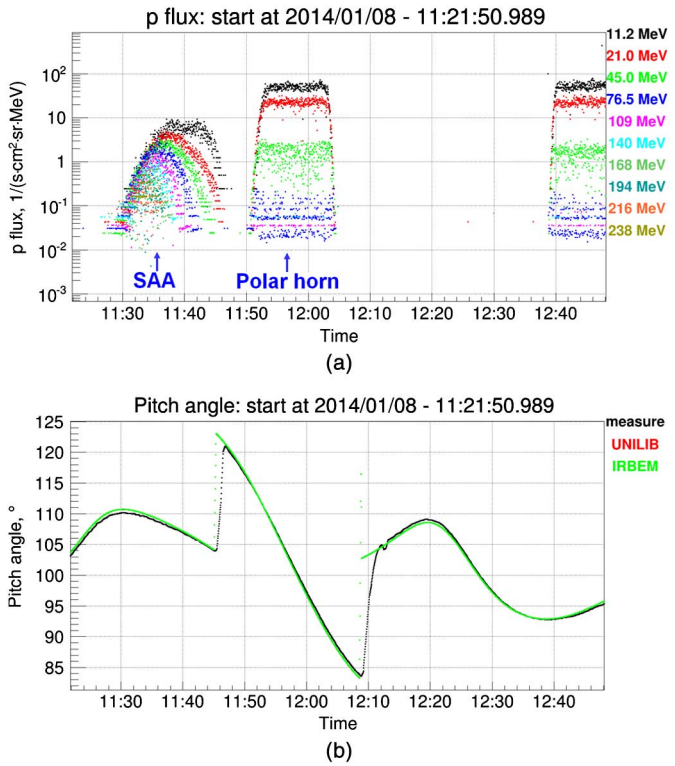

Fig. 2. Proton flux during SPE around January 8th, 2014 (a) and pitch angle variation for the same period of time (b).

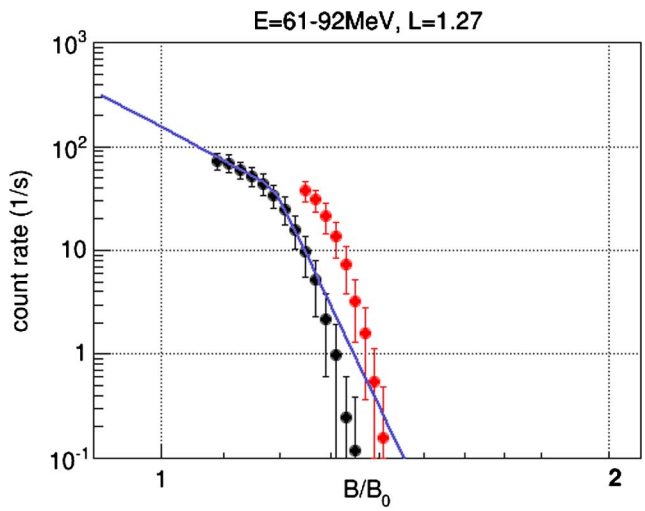

Fig. 3. Proton counts/s measured by the EPT in the 61–92 MeV channel at $\mathbf{L} = 1.27$ as a function of $\boldsymbol{B}/\boldsymbol{B}_0$. The $\boldsymbol{B}/\boldsymbol{B}_0$ coordinate of the RP is 1.1. The two-slopes blue line across black points (night time measurement) aims to show two regimes of proton interactions: with magnetic field (at lower $\boldsymbol{B}/\boldsymbol{B}_0$) and upper atmosphere (at higher $\boldsymbol{B}/\boldsymbol{B}_0$).

Investigations are conducted through GEANT4-based simulations with the ATMOCOSMICS application [11], [12] to confront the observations of Fig. 3 to current models of proton interaction with matter in the upper atmosphere (i.e. East-West asymmetry). Detailed results will be published in a separate paper.

V. Cross-Comparison with RPS and AP8 Data

Inter-species contamination has been discarded from the EPT at design time [7]. The effect of proton angular distribution on

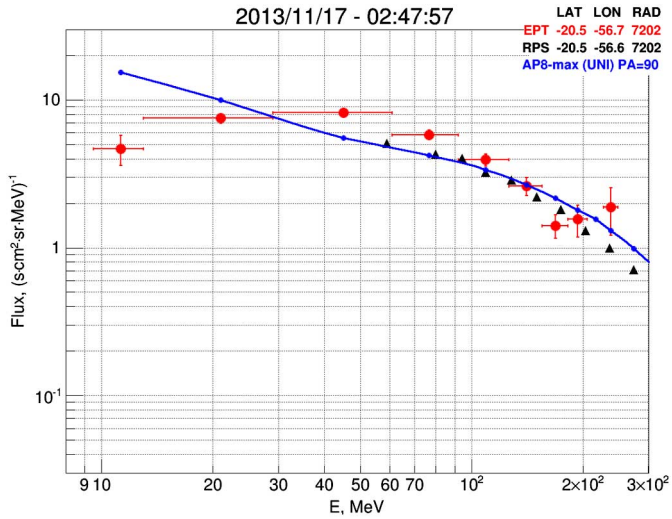

Fig. 4. Single proton spectrum measured by the EPT on Nov. 17th, 2013 as compared to prediction of AP8-MAX Unidirectional and average extrapolated RPS spectrum for position ($-20.5°$LAT, $-56.8°$LON, 7202 km radius) in RP bin.

flux measurements has been analyzed in the previous sections. The results of that analysis may be summarized as follows:

- The Badhwar-Konradi scaling factor in the RP bin at 90° PA amounts to $W_{BK} \cong 3.5$, which means that AP8 omnidirectional fluxes can be converted into unidirectional fluxes at 90° PA by multiplying the omnidirectional fluxes by $3.5/4\pi$;
- Azimuthal angular distribution (East-West asymmetry) is negligible in the RP bin for up to 92 MeV protons (see Fig. 3) and should not affect cross-comparison of results from various instruments and models.

In order to perform cross-comparison of RBSP/RPS and the PROBA-V/EPT measurements, the median daily means of RBSP/RPS fluxes covering 80 days were mapped over a grid in K and $\mathrm{h_{min}}$ (using Olson Pfitzer Quiet magnetic field model) coordinates [13]. Then, predicted PROBA-V locations and pitch angles were mapped into that grid leading to production of flux values for positions as close as possible to those subsequently crossed by the PROBA-V orbit. Typical results of the comparison between EPT and RPS data to AP8-MAX (unidirectional) predictions are illustrated in Fig. 4.

The EPT spectrum is one of the single measurements acquired in the RP bin at boresight orientation towards 90° ($\beta = 90 \pm 3°$). The differential spectra were extracted using a method that assumes isotropic flux in the half-hemisphere facing the instrument aperture. This method allows measuring the average flux of protons over the EPT 52° FOV. The same method was applied to measure the average fluxes over the RPS 26° FOV. The AP8-MAX unidirectional fluxes have been calculated from the Space Environment Information System (SPENVIS), but also cross-checked through evaluation of W_{BK}. They were deduced from integral fluxes calculated at RP center, for energy bin limits corresponding to the ones in the EPT data. A rather good agreement is observed between measurements and AP8 model for 100 MeV protons. The agreement is less satisfactory

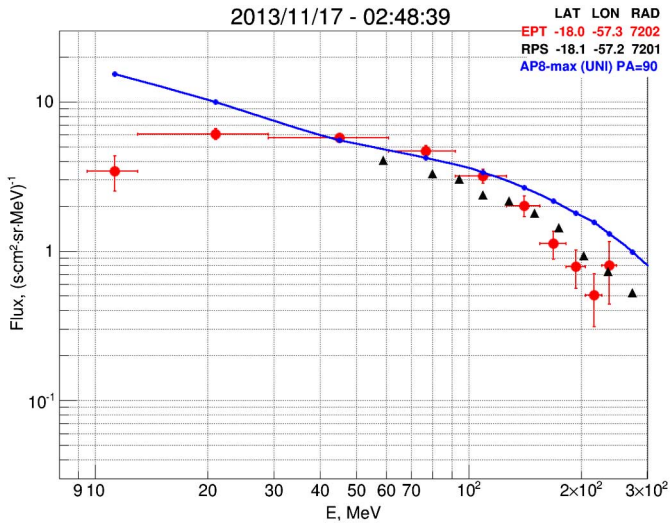

Fig. 5. Single proton spectrum measured by the EPT on Nov. 17th, 2013 as compared to prediction of AP8-MAX Unidirectional and average extrapolated RPS spectrum for position ($-18°$LAT, $-57.3°$LON, 7202 km radius) in RP bin.

at $E < 60$ MeV where the EPT single measurements are either higher or lower than AP8 predictions. These results have been cross-checked using the PAD fitting method since the J_0 parameter of the model corresponds to the maximum value of the FOV-averaged flux for a given channel. As noticed in Fig. 1, that value amounts to 7.8 protons/(cm^{2}s sr MeV) at 45 MeV (the third point of EPT spectrum).

Due to the PAD-averaging operation, one would expect that after many acquisitions in the RP, the EPT average spectra obtained from isotropy assumption over a 52° FOV would be lower than the value obtained by PAD fitting, which should be itself higher than the RPS average spectra. However, the extent of these differences depends on the PAD steepness and the size of the current data set did not allow the further measurement refinements needed to capture such an effect. In order to grab the main factors involved in the variability of cross-comparison results, another spectrum acquired by the EPT inside the RP bin has been compared to RPS and AP8-MAX results. The spectra are shown in Fig. 5.

While good agreement is found between measurements and AP8-MAX for $30 < E < 100$ MeV protons, systematic overestimation of fluxes by the model with regards to measurements is observed at other energies in the RP bin. It should be stressed that AP8-MAX model was based on the data acquired during 3 months of AZUR mission, thereby it would not be expected that this model would fit the data at every position and energy. For energy range of interest (> 10 MeV) AZUR had only 3 broad channels covering $10.4 - 104$ MeV, so it was stated that the model may be inaccurate above 150 MeV [14]. In addition, the slope of the AP8-MAX spectra below 30 MeV in the RP bin is monotonously negative, whereas the EPT has repetitively measured positive-slope spectra at that position. This topic will be further investigated and is outside the scope of this paper. Therefore, validation of all AP8 should be on a case by case basis, at least accounting for position and range of energy, although order of magnitude differences between AP8 and data from science-class instruments should be scarce if angular distribution of fluxes are properly accounted for. With that respect, it has been noticed that the median of AP9 isotropic flux (omnidirectional flux divided by 4π) agrees quite well with the EPT and RPS data shown in Fig. 5, as it predicts 9.15 and 3.04 protons/(cm^{2}s sr MeV) for 40 and 100 MeV, respectively. However, the AP9 which is inherently a unidirectional flux model predicts at 40 MeV a proton unidirectional flux at 90° equal to 43.9 protons/(cm^{2}s sr MeV), which overestimates its measured counterpart (7.8 protons/(cm^{2}s sr MeV)). It is suspected that this over-prediction is linked to the steepness of the AP9 pitch angle distribution shape (Fig. 1). But this hypothesis needs further investigations.

VI. Conclusion

Dividing AP8 omnidirectional fluxes by 4π while evaluating unidirectional fluxes at LEO leads to results that are (by a factor $W_{BK}(B, L, \alpha)$) systematically underestimated. Contamination of energetic proton fluxes by other types of particles and out-of-aperture protons may, in poorly shielded radiation monitors, lead to over 100% flux overestimation. Combination of both factors may explain some of the observed discrepancies between measurements and AP8 prediction, but case by case studies need to be conducted to conclude on AP8 global applicability. The EPT was designed to provide high quality data that may be exploited in such focused studies. Such a methodology allows us to conclude that AP8 does not systematically underestimate $E > 100$ MeV proton fluxes around $B/B_0 = 1.1, L = 1.3$.

Appendix

The procedure applied in reference [15] has been adapted and used to determine the EPT gathering power as described here below.

The coincidence counting rate of a particle telescope for a given physical channel j (that is contamination free to any particle type that it is not dedicated to) at a given time t_0 can be expressed as:

$$C_j(\vec{x}, t_0) = \left(\frac{1}{T}\right) \int_{t_0}^{t_0+T} dt \int_S d\vec{\sigma}\vec{r} \int_\Omega d\omega \times \int_0^{E_{max}} dE\, \varepsilon(E, \omega)\, J(E, \omega, \vec{x}, t) \quad (1)$$

$\vec{x}$ = spatial coordinate of the telescope
T = total observation time
t_0 = time at start of observation
$d\vec{\sigma}$ = element of surface area of the last telescope sensor
$\vec{r}$ = unit vector in direction ω
$d\vec{\sigma}\vec{r}$ = effective element of area looking into ω
$d\omega = \sin(\theta)\, d\theta\, d\phi$, element of solid angle (θ polar angle, ϕ azimuth)
E = energy of the incident particle
ε = detection efficiency for the particles getting into the instrument through the aperture

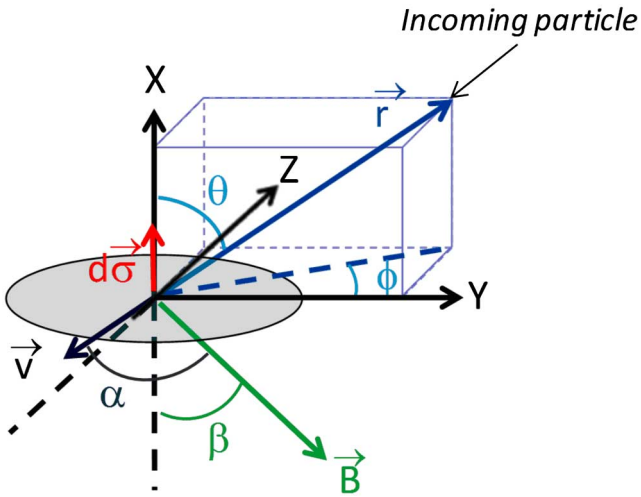

Fig. 6. Definition of the coordinate system used in the particle simulation procedure. The vector $\vec{v}$ represents the velocity of the particle. It defines the particle pitch angle α in the given reference frame.

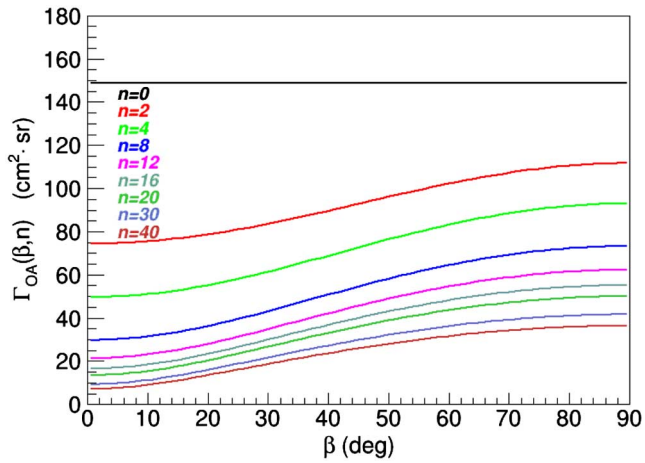

Fig. 7. Gathering power of the opening aperture as a function of boresight orientation β for various exponents of the PA distribution n.

J = spectral intensity (s^{-1} cm^{-2} sr^{-1} MeV^{-1}), i.e. differential flux as seen from the aperture

If it is assumed that within the obsertion time J is independent on t and separates into

$$J\left(E,\omega,\vec{x},t\right)=J_0\left(E,\vec{x},t_0\right)F\left(E,\omega\right) \tag{2}$$

where $F(E,\omega)$ for the proton flux is assumed to be of the type $F(E,\omega) = sin^{n(E)}(\alpha)$ where α is the angle between the incoming direction of the particle and the magnetic field in an inertial reference frame and the anisotropy factor n is supposed to vary with energy; then (1) becomes

$$C_j\left(\vec{x},t_0\right)=\int_0^{E_{max}}J_0\left(E,\vec{x},t_0\right)\times\left[\int_\Omega d\omega\int_S d\vec{\sigma}\vec{r}\,\varepsilon\left(E,\omega\right)F\left(E,\omega\right)\right]dE \tag{3}$$

In case of discrete energy steps in the definition of the incident energy channels of the telescope (for the EPT instrument 11 channels are defined), this expression becomes:

$$C_j\left(\vec{x},t_0\right)=\sum_{i=1}^{11}J_0\left(i,\vec{x},t_0\right)\left[\int_\Omega d\omega\int_S d\vec{\sigma}\vec{r}\,\varepsilon_i\left(\omega\right)F_i\left(\omega\right)\right] \tag{4}$$

where $J_0(i,\vec{x},t_0)=\int_{E_i min}^{E_i max}J_0(E,\vec{x},t_0)dE$ represents the integrated flux within the given energy bin $[E_i\min, E_i\max]$.

For detector types like the EPT, where a given incident energy range (i) defines majorly the counting rate in a corresponding physical channel (j), this equation may be simplified into (the subscripts i and j denoting the channels are dropped):

$$C\left(\vec{x},t_0\right)=J_0\left(i,\vec{x},t_0\right)\left[\int_\Omega d\omega\int_S d\vec{\sigma}\vec{r}\,\varepsilon\left(\omega\right)F\left(\omega\right)\right] \tag{5}$$

and the expression in brackets of eq. (3) is the so-called energy dependent gathering power of the telescope when the incident flux intensity has an angular dependence given by $F(\omega)$.

$$\Gamma_F=\int_\Omega d\omega\varepsilon\left(\omega\right)F\left(\omega\right)\int_S d\vec{\sigma}\overrightarrow{r} \tag{6}$$

In the case of EPT, the efficiency $\varepsilon(\omega)$ is approximated by its average value over the instrument 26° half-FOV angle. The average efficiency is obtained by GEANT4 simulation technique applied to 5–300 MeV protons. Within this method, particle tracks are initiated at randomly selected position on the opening aperture, with an initial momentum direction that is generated accounting for the assumed angular distribution as described hereunder. The protons are then tracked through the instrument materials and the events are classified in the various physical channels (when coincident hits in sensors and deposited energy threshold conditions are fulfilled). The gathering power is then given by:

$$\Gamma_F=\frac{\text{number of trajectories detected}}{\text{total number of trajectories chosen}}\Gamma_{OA} \tag{7}$$

where Γ_{OA} is the pure gathering power of the opening aperture (planar aperture from which the particles are launched). It depends on the intensity angular distribution $F(\omega) = F(\theta,\phi)$ and therefore on n and the looking direction (β) of the instrument with respect to the magnetic field. It is calculated by numerical integration as

$$\Gamma_{OA}\left(n,\beta\right)=\int_{\theta=0}^{\pi/2}\int_{\phi=0}^{2\pi}\sin\left(\theta\right)d\theta d\phi\int_S d\sigma\,cos\left(\theta\right)F\left(\theta,\phi\right) \tag{8}$$

where θ and ϕ are the polar and azimuthal angles as defined in the reference system shown in Fig. 6. The reference system is taken so that the X axis is in the same direction as $d\vec{\sigma}$, and the magnetic field vector $\vec{B}$ is in the plane defined by XY.

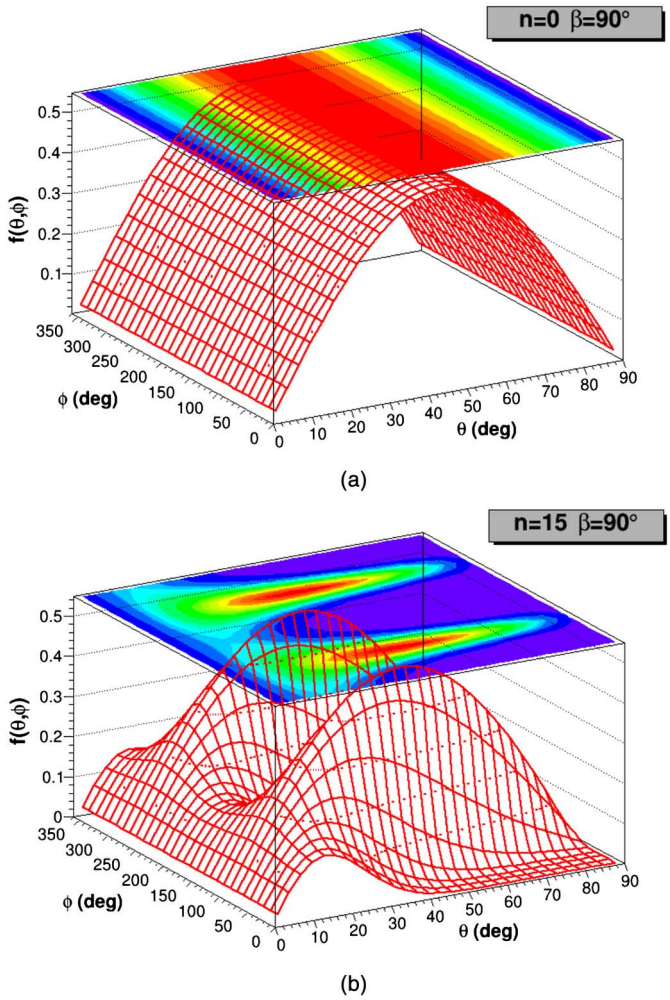

Fig. 8. Representation of the function $\boldsymbol{f}(\boldsymbol{\theta},\phi) = \cos(\boldsymbol{\theta})\boldsymbol{F}(\boldsymbol{\theta},\phi)\sin(\boldsymbol{\theta})$ for two combinations of exponent of the PAD n and boresight orientation β : (a) $n = 0$ and $\beta = 90°$, (b) $n = 15$ and $\beta = 90°$.

Within this reference system $\vec{B} = B\begin{pmatrix} -\cos(\beta) \\ \sin(\beta) \\ 0 \end{pmatrix}$ and $\vec{v} = -v\begin{pmatrix} \cos(\theta) \\ \sin(\theta)\cos(\phi) \\ \sin(\theta)\sin(\phi) \end{pmatrix}$ and the resulting particle PA α is then given after calculating the scalar product of $\vec{B}$ and $\vec{v}$ by

$$\cos(\alpha) = \cos(\theta)\cos(\beta) - \sin(\beta)\sin(\theta)\cos(\phi) \qquad (9)$$

With this the gathering power of the opening aperture (Eq. (6)) can be calculated by assuming $F(\theta,\phi) = sin^n(\alpha)$ and using (9). Variations of the gathering power of the opening aperture as a function of n and β is given in Fig. 7.

For all the energy channels, the angle-averaged efficiency (see fraction in (7)), hereafter labelled ϵ_{CH}, 24 billions of proton events in the energy range 5–300 MeV have been simulated for pitch angle distributions with $n = 0 - 60$ (in steps of $\Delta n = 1$) and $\beta = 25° - 90°$ (in steps of $\Delta\beta = 5°$).

Several rules were followed while initiating the simulation of the trajectories [15]:

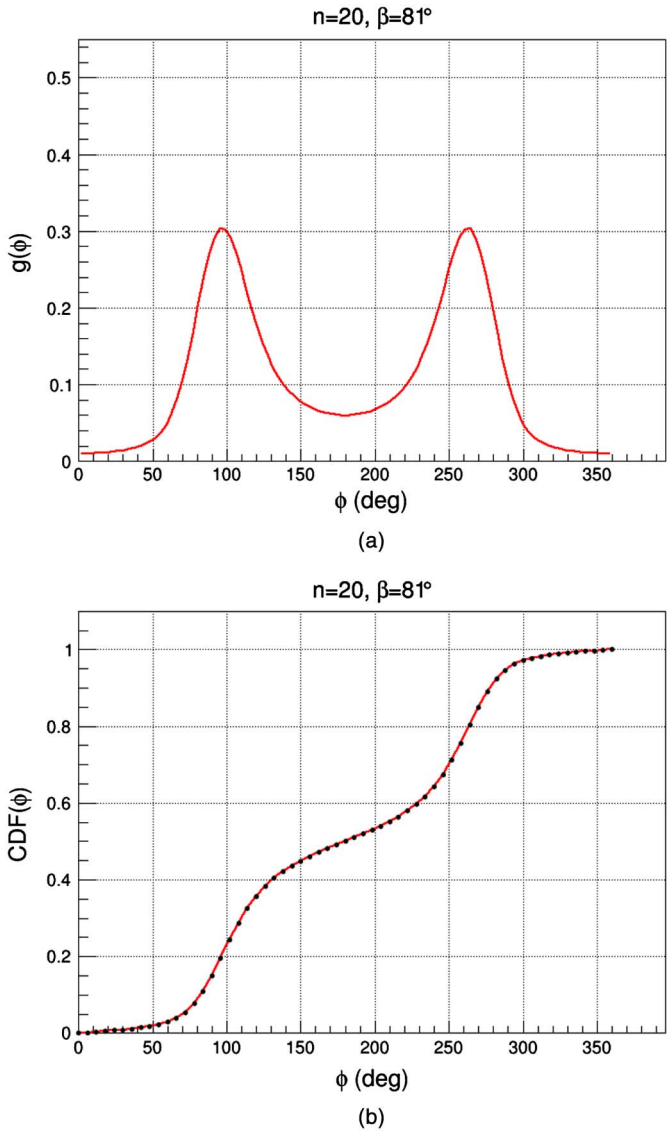

Fig. 9. For a given PAD exponent n and boresight orientation β, (a) the PDF (not normalized) and (b) the corresponding CDF for the variable $\boldsymbol{\phi}$.

a) By choosing a random point on the opening aperture, equal areas should have equal weights. For a circular aperture $d\sigma = \frac{1}{2}dr^2 d\varphi$ and thus random r^2 and φ are chosen.
b) To choose trajectories corresponding to the intensity incident on the aperture (β and n are fixed), the element of area $d\sigma$ centered on the point picked in a) is considered and the weighted solid angle is calculated. The incident directions are weighted not only by $F(\omega)$ but also by a factor $\cos(\theta)$ coming from $d\vec{\sigma}\,\overrightarrow{r} = d\sigma\cos(\theta)$ (cf(6)). The weighted solid angle is given by:

$$\begin{aligned} dN &= \cos(\theta)\,F(\theta,\phi)\sin(\theta)\,d\theta\,d\phi \\ &= \frac{1}{2}F(\theta,\phi)\,d\,cos^2(\theta)\,d\phi \end{aligned} \qquad (10)$$

and $F(\theta,\phi) = sin^n(\alpha)$ with α defined as in (9).

In an isotropic field where $F(\theta,\phi) = 1$, this would result in choosing random ϕ and random $\cos^2(\theta)$. In an anisotropic field,

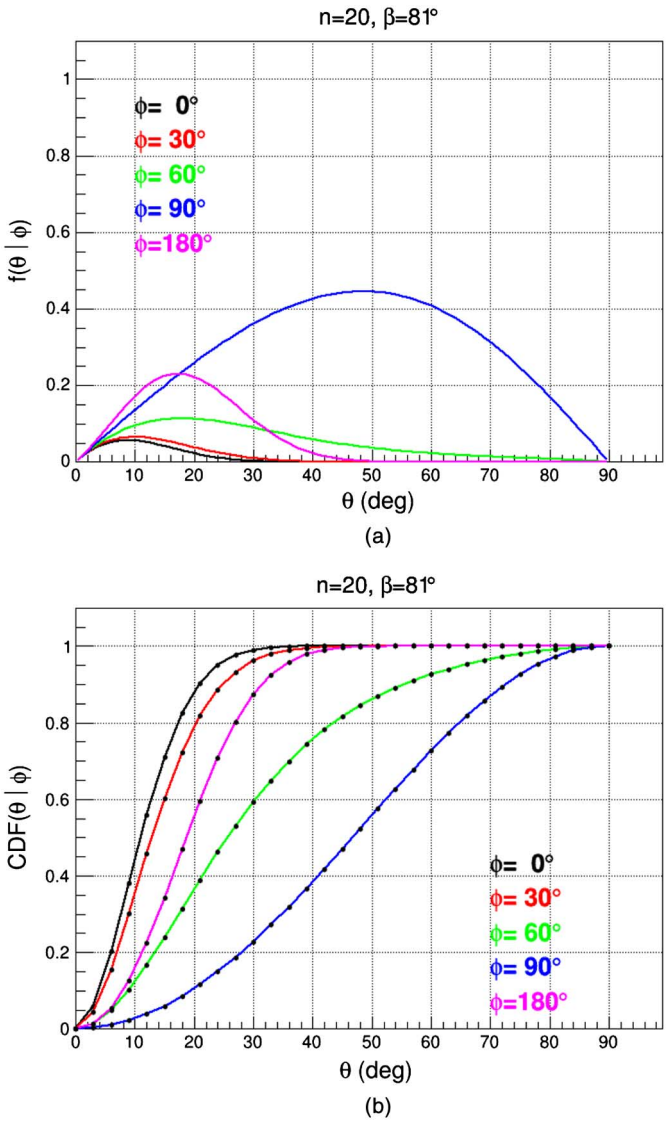

Fig. 10. For a given PAD exponent n and boresight orientation β, and various ϕ, (a) the PDF (not normalized) and (b) the corresponding CDF for the variable $\boldsymbol{\theta}$.

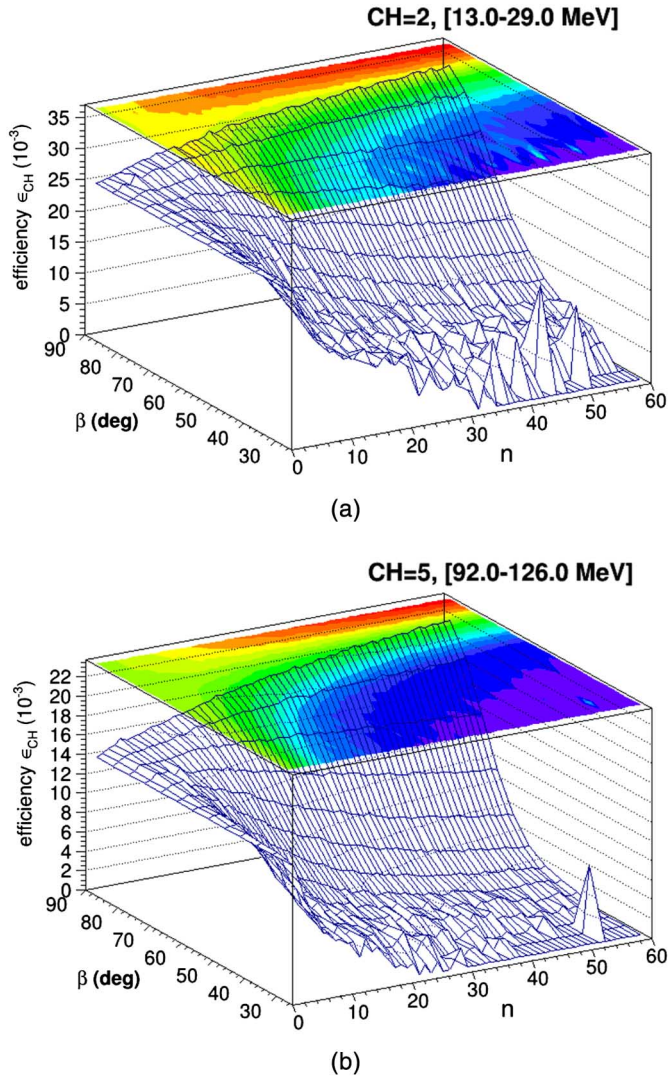

Fig. 11. Efficiency of channel 2 and 5 as a function of exponent of the PAD n and boresight orientation β, for the incident proton energy ranges to which these channels are the most efficient: (a) channel 2, 13–29 MeV and (b) channel 5, 92–126 MeV.

the situation is more complex and the selection of (θ, ϕ) is done in two steps.

Equation (9) is rewritten using Bayes' theorem in the following way:

$$dN = f\,(\theta,\phi)\,d\theta\,d\phi = f\,(\theta|\phi)\,d\theta\;g\,(\phi)\;d\phi \qquad (11)$$

where $f(\theta,\phi) = \cos(\theta)F(\theta,\phi)\sin(\theta)$ and $\mathrm{f}(\theta|\phi)$ is considered to represent the probability density function (PDF) of θ for a given ϕ and $g(\phi)$ represents the PDF of ϕ and is given by the integration of $f(\theta,\phi)$ over the range of θ:

$$g\,(\phi) = \frac{1}{\pi/2}\int_{\theta=0}^{\pi/2} f\,(\theta,\phi)\,d\theta \qquad (12)$$

Fig. 8 represents the function $f(\theta,\phi)$ for two combinations of n and β. One recognizes the shape in $\cos^2(\theta)$ and the constant in ϕ in the case of isotropic flux ($n = 0$).

For each set of (n,β), the PDF and the cumulative distribution function (CDF) are generated for the variable ϕ and θ (Fig. 9 and Fig. 10). During the trajectory simulation, first a random ϕ is selected with respect to its CDF and then only the corresponding θ is generated with respect to its CDF.

Fig. 11 shows the variation of the efficiency ϵ_{CH} of physical channel 2 and 5 as a function of n and β for the incident proton energy ranges to which $\mathrm{PC} = 2$ and 5 show the highest efficiency. When β is below 50° and n very large, then the amount of flux detected by the telescope is very low and this is reflected in the large statistical fluctuations of the simulated efficiency. It must be mentioned that in order to accelerate the simulation, trajectories with $\theta > 26°$ were not tracked through the detector as they are outside the viewing angle of the instrument. The gathering power Γ_{OA} was adapted to this situation by restricting the integral over θ in eq. (6) to 26°.

The count rates of detected protons in off-pointing positions for a given physical channel (energy bin) are then fitted by taking into account the corresponding efficiency matrix

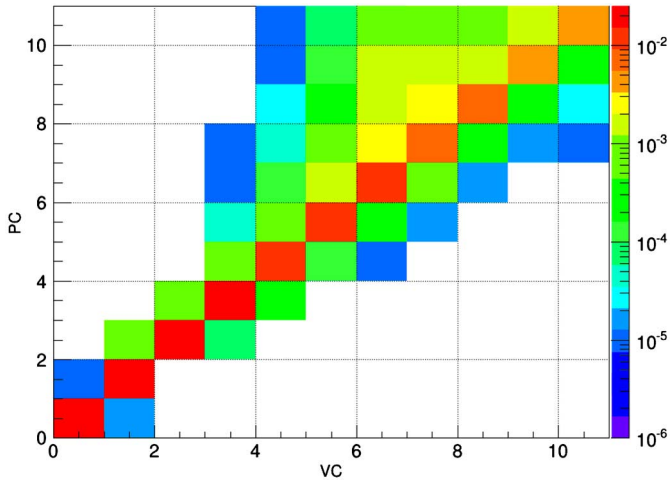

Fig. 12. Graphical representation of the proton efficiency matrix for $n = 0$. PC labels the 11 proton physical channels used in the EPT data analysis and VC represents the virtual channels which correspond to an incident proton energy bin (cf Fig. 13 for their values).

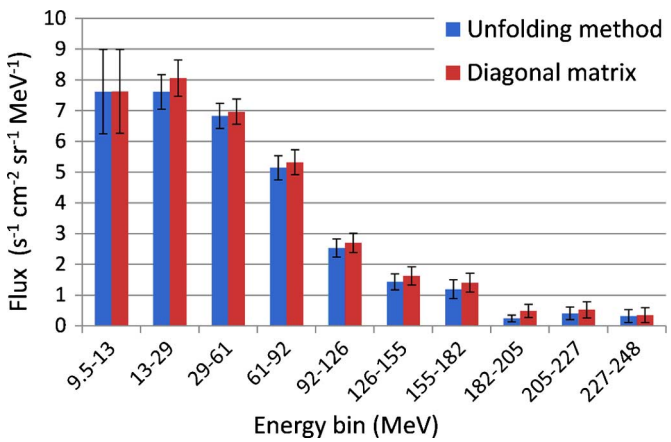

Fig. 13. Proton spectrum obtained by the two analysis methods. In blue: the complete efficiency matrix is considered to unfold the measured spectrum, in red: only the diagonal part of the matrix is considered to translate the count rates into differential fluxes.

$\epsilon_{CH}(n,\beta)$. In the measured distribution of count rates as a function of β, the points where grouped by steps of 5° and averaged.

Additional remarks:

The proton channels for the EPT have been defined in such a way that the efficiency matrix $\epsilon_{CH}(n,\beta)$ is highly diagonal as can be seen in Fig. 12. For $\mathrm{PC} = 1 - 6$, the dedicated proton energy population defines by more than 90% the number of particles detected in a given channel.

Fig. 13 represents a reconstructed proton spectrum if two different methods for spectra extraction are used. In blue: the complete efficiency matrix is considered to unfold the measured spectrum, in red: only the diagonal part of the matrix is considered to translate the count rates into differential fluxes. It can be observed that within the given statistical variations, there is no difference between both spectra.

From these efficiency matrices $\epsilon_{CH}(n,\beta)$ and the corresponding gathering powers of the opening aperture $\Gamma_{OA}(n,\beta)$ it can be deduced by how much the directional flux $J_0(\vec{x},t_0)$ is

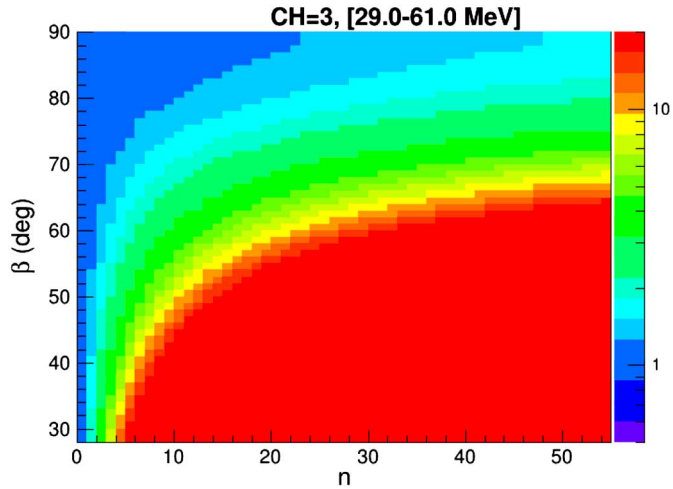

Fig. 14. Representation of the correction factor $\boldsymbol{R}_\Gamma$ (see text for definition) as a function of exponent of the pitch angle distribution n and boresight orientation β.

under- or overestimated if the isotropic flux assumption is assumed. Fig. 14 shows the ratio $\mathrm{R}_\Gamma(n,\beta)$ between the isotropic flux gathering power $\Gamma_F(n=0,\beta) = \epsilon_{CH}(0,\beta)\Gamma_{OA}(0,\beta)$ and the anisotropic flux gathering power $\Gamma_F(n,\beta)$. It is a correction factor that must be applied to the deduced fluxes obtained under the isotropic flux assumption in order to obtain the directional fluxes for a given β taking into account that the flux anisotropy factor is n. It can be observed that if $80° < \beta < 90°$ and $\mathrm{n} < 30$ then J_0 measured with a given β and deduced under the isotropic flux assumption corresponds to the effective directional flux within about 30%. The factor R_Γ is always higher than one which means that the flux is underestimated if $\Gamma_F(n=0,\beta)$ is applied to the counts $C(\vec{x},t_0)$ to recover $J_0(\vec{x},t_0)$.

ACKNOWLEDGMENT

The authors are grateful to C. Baijot, D. Gerrits, S. Ilsen, K. Mellab, J. Naudet, C. Semaille, E. Tilmans, and J. Van Hove for authorizing, preparing and performing the off-pointing maneuvers without which PAD measurements at PROBA-V positions would not have been performed. Special thanks to the PROBA-V/EPT team at B. USOC and QinetiQ Space for taking care of the data. The CSR team also thanks P. Coquay, J. Nijskens, H. Verbeelen, and W. Verschueren at the Belgian Science Policy–Space Research and Applications (BELSPO) for support to the PRODEX project entitled "PROBA-V/EPT–Data Exploitation", ESA Contract C4000107617.

REFERENCES

[1] S. L. Huston, *Space Environments and Effects: Trapped Proton Model*. Huntington Beach, CA, USA: The Boeing Company, Jan. 2002, NAS8-98218.

[2] M. A. Xapsos, S. L. Huston, J. L. Barth, and E. G. Stassinopoulos, "Probabilistic model for low-altitude trapped-proton fluxes," *IEEE Trans. Nucl. Sci.*, vol. 49, no. 6, pp. 2776–2781, Dec. 2002.

[3] D. Heynderickx, M. Kruglanski, V. Pierrard, J. Lemaire, M. D. Looper, and J. B. Blake, "A low altitude trapped proton model for solar minimum conditions based on SAMPEX/PET data," *IEEE Trans. Nucl. Sci.*, vol. 46, no. 6, pp. 1475–1480, Dec. 1999.

[4] J. Cabrera *et al.*, "Fluxes of energetic protons and electrons measured on board the oersted satellite," *Annales Geophysicae*, vol. 23, pp. 2975–2982, 2005.

[5] G. D. Badhwar and A. Konradi, "Conversion of omnidirectional proton fluxes into a pitch angle distribution," *J. Spacecraft Rockets*, vol. 27, no. 3, pp. 350–352, 1990.

[6] M. Siegl, H. D. R. Evans, E. J. Daly, G. Santin, P. J. Nieminen, and P. Bühler, "Inner belt anisotropy investigations based on the standard radiation environment monitor (SREM)," *IEEE Trans. Nucl. Sci.*, vol. 57, no. 4, pp. 2017–2023, Aug. 2010.

[7] M. Cyamukungu and Gh. Grégoire, "The energetic particle telescope (EPT) concept and performances," in *Proc. 4th Solar Physics and Space Weather Instrumentation Conf.*, Oct. 2011, vol. 8148, ISBN: 9780819487582.

[8] M. Kruglanski and J. Lemaire, Trapped Proton Anisotropy at Low Altitudes Belgian Institute for Space Aeronomy (BISA), Brussels, Belgium, Tech. Note 6, TREND-3 Rep., Apr. 1996.

[9] J. V. Rodriguez, J. C. Krosschell, and J. C. Green, "Intercalibration of goes 8–15 solar proton detectors," *Space Weather*, vol. 12, no. 1, pp. 92–109, Jan. 2014.

[10] H. M. Fischer, V. W. Auschrat, and G. Wibberenz, "Angular distribution and energy spectra of protons of energy $5 \leq E \leq 50$ at the lower edge of the radiation belt in equatorial latitudes," *J. Geophys. Res.*, vol. 82, no. 4, pp. 537–547, Feb. 1977.

[11] S. Agostinelli *et al.*, "GEANT4–A simulation toolkit," *Nucl. Instrum. Methods Phys. Res. A*, vol. 506, pp. 250–303, 2003.

[12] L. Desorgher, E. O. Flückiger, M. Gurtner, M. R. Moser, and R. Bütikofer, "Atmocosmics: A geant 4 code for computing the interaction of cosmic rays with the earth's atmosphere," *Int. J. Modern Phys. A*, vol. 20, pp. 6802–6804, Jan. 2005.

[13] G. P. Ginet *et al.*, "AE9, AP9 and SPM: New models for specifying the trapped energetic particle and space plasma environment," *Space Sci. Rev.*, vol. 179, no. 1–4, pp. 579–615, Nov. 2013.

[14] D. M. Sawyer and Vette, "AP-8 trapped proton environment for solar maximum and solar minimum," National Space Science Data Center, Greenbelt, MD, USA, Rep. 76–06, 1976.

[15] J. D. Sullivan, "Geometrical factor and directional response of single and multi-element particle telescopes," *Nucl. Instrum. Methods Phys. Res. A*, vol. 95, no. 1, pp. 5–11, Aug. 1971.